

Symmetry Properties of the Phase of Coexistence of Superconductivity and Antiferromagnetism in 2D Systems with Strong Electron Correlations

V. V. Val'kov and A. O. Zlotnikov

Kirensky Institute of Physics, Siberian Branch, Russian Academy of Sciences, Krasnoyarsk, 660036 Russia

e-mail: vvv@iph.krasn.ru

Received April 30, 2015

Abstract—Using the diagram technique for Hubbard operators, the effect of quasi-two-dimensionality and hybridization of the $4f$ electrons of cerium ions and p electrons of indium ions on the properties of the antiferromagnetic, superconducting, and mixed phases in heavy-fermion intermetallic compounds of cerium is studied. It is shown that taking into account quasi-two-dimensionality, low-energy hybridization processes renormalize the antiferromagnetic and superconducting order parameters in the broken time-reversal symmetry phase. Estimates of the critical temperatures of antiferromagnetic ordering and Cooper instability, obtained by the developed approach, are in good agreement with experimental data for cerium-based intermetallic compounds.

Keywords: superconductivity, antiferromagnetism, two-dimensional systems, strong electron correlations, heavy fermions, cerium-based intermetallic compounds, periodic Anderson model

DOI: 10.1134/S1027451016010195

INTRODUCTION

It is known that Cooper pairing occurs between electrons with states which transform into each other under the time-reversal operation. In materials with long-range magnetic order, such symmetry is broken. This is one of the reasons for the competition between superconductivity and magnetic ordering. In ferromagnetic materials, for example, singlet superconductivity is either suppressed or leads to the transformation of ferromagnetic ordering, in particular, into a spiral magnetic structure [1].

Fundamentally different behavior is observed in antiferromagnetic materials. The symmetry in them is broken with respect to time reversal; however, states, which are connected to each other by successive operations of time reversal and translation to a vector connecting ions of different sublattices in the magnetic unit cell, have the same energy [2]. These states can participate in the formation of the Cooper instability in antiferromagnetic compounds. With this in mind, it is said that antiferromagnetic superconductors have a special type of symmetry.

There are many examples of materials where superconductivity occurs in the presence of long-range antiferromagnetic order. These include, for example, the rare-earth ternary borides and chalcogenides, some cuprate high-temperature superconductors, iron pnictides, and heavy-fermion compounds. In recent years, compounds based on rare-

earth intermetallic compounds (for example, CeIn_3 , CeRhIn_5 , or CePt_2In_7 from the group $\text{Ce}_n\text{T}_m\text{In}_{3n+2m}$) have attracted considerable interest. In these compounds, a microscopically homogeneous phase of the coexistence of superconductivity and antiferromagnetism (mixed phase), that is, the broken time-reversal symmetry phase, is observed at low temperatures [3, 4]. There are several reasons that determine the relevance of the study of superconductivity with time-reversal symmetry broken by magnetic ordering. First, the proximity of the superconducting phase to the antiferromagnetic phase in the phase diagram and the emergence of a mixed phase of antiferromagnetism and superconductivity in a number of materials are the most important properties of high-temperature superconductors. Second, the relationship between the two types of ordering ensures that the external influence on, for example, the magnetic subsystem of such materials makes it possible to control their superconducting properties. Third, it was recently suggested that in layered compounds with trigonal or hexagonal symmetry, the coexistence of chiral superconductivity and noncollinear magnetic order contributes to the formation of Majorana bound states [5, 6].

Intensive experimental studies of CeRhIn_5 led to the determination of a number of unusual properties of this heavy-fermion compound. At atmospheric pressure, this compound is an antiferromagnet with a Néel temperature of 3.8 K [7]. The application of

external pressure leads to the suppression of antiferromagnetism and causes the emergence of superconductivity. A number of experiments on nuclear quadrupole resonance and neutron diffraction prove that in CeRhIn₅, a microscopically homogeneous phase of coexistence of superconductivity and antiferromagnetism occurs up to the critical pressure, at which the antiferromagnetism is destroyed [8, 9].

The mechanism of superconductivity in cerium heavy-fermion systems is still a subject of intense debate. One of the possible nonphonon mechanisms is a magnetic mechanism caused by the magnetic nature of interaction and spin fluctuations [10, 11]. Alternative nonphonon mechanisms of superconductivity are directly associated with possible fluctuations of non-magnetic nature near the quantum critical point of heavy-fermion metals. In [12], it is assumed that the appearance of the Cooper instability is associated with strong valence fluctuations. With respect to cerium heavy-fermion compounds, it has often been suggested that the formation of superconducting pairs is due to fluctuations near the local quantum critical point, at which the Kondo regime is established upon the destruction of antiferromagnetism [13]. Recently, however, based on the quantum Monte Carlo method for the periodic 2D Anderson model with frustrated hybridization interaction, it was shown that antiferromagnetic spin fluctuations made the main contribution to the *d*-wave superconductivity emergence in compounds Ce-115 (CeRhIn₅, CeCoIn₅) [14].

A significant feature of cerium compounds of the CeRhIn₅ type is their quasi-two-dimensional structure [7]. It is known that for a quasi-two-dimensional Heisenberg antiferromagnet, the Néel temperature is determined by the formula $T_N = \pi J / (\ln(J/K) + c)$, where J is the parameter of exchange between the nearest ions in the *xy* plane, parameter K sets the value of the exchange interaction between the nearest neighbors along the *z* axis, and c is a constant depending on the type of lattice [15]. This equation indicates a decrease in the transition temperature compared with the isotropic case. For CeRhIn₅, the exchange parameters were estimated, $J = 0.74$ meV and $K = 0.1$ meV, based on experimental data on neutron spectroscopy and using the Heisenberg model [16]. The consideration of hybridization can renormalize these parameters. In this context, estimation of the Néel temperature for quasi-two-dimensional heavy-fermion antiferromagnets, taking into account the hybridization process, is an important task.

The periodic Anderson model is commonly used as a base model for the heavy-fermion systems, especially in the regime of variable valence [17]. Based on obtaining an effective Hamiltonian for the periodic Anderson model, it is demonstrated that the exchange interaction between localized electrons can be induced by high-energy hybridization processes, while low-energy contributions characterize the regime of

mixed valence [18]. This exchange interaction leads to the induction of Cooper pairing and the appearance of a mixed phase [19]. This determines the nature of the magnetic mechanism of the Cooper instability with *d*-wave pairing in two-dimensional systems of rare-earth elements with broken symmetry with respect to the time-reversal operation [20].

In the present paper, the temperature dependences of the order parameters in the antiferromagnetic and mixed phases with broken time-reversal symmetry are determined for quasi-two-dimensional intermetallic compounds of cerium within the extended periodic Anderson model, based on the diagram technique in atomic representation [21, 22]. In developing the theory, we take into account that the superconducting and antiferromagnetic orderings are induced by the same exchange interaction in the subsystem of localized electrons. Accounting for hybridization in the theory of the mean exchange field leads to a rather high critical temperature for the antiferromagnetic phase [23]; therefore, in this paper, the necessary renormalization is carried out based on the spin-wave theory of a heavy-fermion antiferromagnet. The Néel temperature and the temperature of transition to the broken time-reversal symmetry phase, which is characterized by the coexistence of superconductivity and antiferromagnetism, are in good agreement with the values determined experimentally for cerium systems (for example, CeRhIn₅). The advantages of the developed theory in comparison with other works in this field lie in the fact that description of the antiferromagnetic phase is carried out within the framework of spin-wave theory taking into account hybridization between localized and itinerant electrons, without using the concept of fully localized electrons. This approach gives a unified description of both the antiferromagnetic and mixed phase in heavy-fermion systems at finite temperatures.

MODEL AND METHOD

We write the Hamiltonian of the effective periodic Anderson model, which takes into account the exchange interaction of quasi-localized electrons in a subsystem, as

$$\widehat{H}_{\text{eff}} = \widehat{H}_0 + \widehat{H}_{\text{mix}} + \widehat{H}_{\text{exch}}. \quad (1)$$

The term of the Hamiltonian

$$\widehat{H}_0 = \sum_{j=1,2} \left\{ \sum_{\mathbf{k}\sigma} \xi_{\alpha\mathbf{k}} \alpha_{j\mathbf{k}\sigma}^\dagger \alpha_{j\mathbf{k}\sigma} + \sum_{\mathbf{k}\sigma} \xi_{\beta\mathbf{k}} \beta_{j\mathbf{k}\sigma}^\dagger \beta_{j\mathbf{k}\sigma} + \sum_{f\sigma} \xi_{\sigma}^F X_{ff}^{\sigma\sigma} + \sum_{g\sigma} \xi_{\sigma}^G Y_{gg}^{\sigma\sigma} \right\}, \quad (2)$$

describes noninteracting localized and itinerant electrons in a lattice with two antiferromagnetic sublattices *F* and *G*. To describe the quasi-two-dimensionality of heavy-fermion intermetallic compounds, we

introduced summation over index $j = 1, 2$, which numbers the plane along the z axis in the unit cell. A G -type antiferromagnetic structure (classification [24]) will be considered in the paper. The Hamiltonian \hat{H}_0 is diagonal in the representation of Bogolyubov operators $\alpha_{j\mathbf{k}\sigma}$ and $\beta_{j\mathbf{k}\sigma}$, which act on the itinerant states in the lower and upper antiferromagnetic subbands, respectively. The formation of two subbands is caused by doubling of the unit cell and a reduction in the Brillouin zone upon the appearance of long-range antiferromagnetic order. The initial energy values of Bogolyubov quasiparticles in K space are determined by equations $\xi_{\alpha\mathbf{k}} = \xi_{\mathbf{k}} + \Gamma_{\mathbf{k}}$ and $\xi_{\beta\mathbf{k}} = \xi_{\mathbf{k}} - \Gamma_{\mathbf{k}}$. The following designations are used: $\xi_{\mathbf{k}} = \varepsilon_0 + t_{\mathbf{k}} - \mu$, ε_0 is the on-site energy of an itinerant electron, μ is the chemical potential, and functions $t_{\mathbf{k}}$ and $\Gamma_{\mathbf{k}}$ are determined as the Fourier transforms of hopping integrals in the sublattices and between them. It is assumed that electron hopping is only possible in the xy plane, and the parameter of hopping between the nearest neighbors along the z axis is negligible.

The Hubbard operator $X_m^{nn'}$, belonging to a Wannier cell m is expressed in terms of atomic states in the usual way, that is, $X_m^{nn'} = |n; m\rangle\langle m; n'|$. The action of the Hubbard operator on an arbitrary state of cell m is given by expression $X_m^{nn'} |s; m\rangle = \delta_{ns} |n; m\rangle$, where δ_{ns} is the Kronecker delta. Notation $|0; m\rangle$ determines the state without electrons in cell m . The state with one electron at a site, having a spin projection of $\sigma = \uparrow, \downarrow$, is designated as $|\sigma; m\rangle$. The algebra of the Hubbard operators and their commutation relations are described in more detail in the original paper [25]. The finite value of the Coulomb repulsion of electrons localized at the site is considered by perturbation theory, whereby the exchange interaction between localized electrons was induced in the system [18]. Sites designated by index f refer to the F -sublattice, for which $\langle S_f^z \rangle = R > 0$ in the presence of antiferromagnetism. The sites of the G sublattice are numbered by index g , and for them the equality of $\langle S_g^z \rangle = -R$ is true.

The energy of localized levels for the F - and G sublattices can be written as

$$\xi_{\sigma}^F = E_0 - \mu - \frac{(J_0 + K_0)}{2} \left(\frac{n_L}{2} + \eta_{\sigma} R \right), \quad \xi_{\sigma}^G = \xi_{\sigma}^F. \quad (3)$$

Equation (3) takes into account a mean-field "exchange" correction to the initial energy of localized electrons E_0 ; n_L is the average number of electrons at a localized level, J_0 is the total value of the exchange interaction between an f electron and electrons occupying neighboring sites in the xy plane, and K_0 is the sum of the exchange parameters of the f electron and its nearest neighbors along the z axis. Function η_{σ} , dependent on σ , is determined in the usual way: $\eta_{\sigma} = 1$ if $\sigma = \uparrow$, and $\eta_{\sigma} = -1$, if $\sigma = \downarrow$.

The operator of the hybridization interaction after expansion over quasi-momenta is convenient to represent in the form

$$\hat{H}_{\text{mix}} = \sum_{j=1,2} \sum_{\mathbf{k}\sigma} \hat{C}_{j\mathbf{k}\sigma}^{\dagger} \hat{A}_{\mathbf{k}} \hat{C}_{j\mathbf{k}\sigma}, \quad (4)$$

where $\hat{C}_{j\mathbf{k}\sigma}^{\dagger} = (\alpha_{j\mathbf{k}\sigma}^{\dagger}, \beta_{j\mathbf{k}\sigma}^{\dagger}, X_{j\mathbf{k}\sigma}^{\dagger}, Y_{j\mathbf{k}\sigma}^{\dagger})$, $\hat{A}_{\mathbf{k}}$ is the block matrix, that is

$$\hat{A}_{\mathbf{k}} = \frac{1}{\sqrt{2}} \begin{bmatrix} \hat{O} & \hat{B}_{\mathbf{k}} \\ \hat{B}_{\mathbf{k}}^{\dagger} & \hat{O} \end{bmatrix}, \quad \hat{B}_{\mathbf{k}} = \begin{bmatrix} V_{\mathbf{k}} + W_{\mathbf{k}} & V_{\mathbf{k}} + W_{\mathbf{k}} \\ W_{\mathbf{k}} - V_{\mathbf{k}} & V_{\mathbf{k}} - W_{\mathbf{k}} \end{bmatrix} \quad (5)$$

In the definition of matrix (5), \hat{O} is the zero matrix 2×2 , and $V_{\mathbf{k}}$ and $W_{\mathbf{k}}$ are the Fourier transforms of the hybridization integrals in the xy plane in the sublattices and between them, respectively.

The effective antiferromagnetic coupling between localized electrons is described by the third term of the Hamiltonian, which can be written as

$$\begin{aligned} \hat{H}_{\text{exch}} = & \sum_{j=1,2} \sum_{\langle fg \rangle} J_{fg} \left(\Delta \mathbf{S}_{jf} \Delta \mathbf{S}_{jg} - \frac{1}{4} \Delta \hat{N}_{jf} \Delta \hat{N}_{jg} \right) \\ & + \sum_{i \neq j} \sum_{\langle fg \rangle} K_{fg} \left(\Delta \mathbf{S}_{if} \Delta \mathbf{S}_{jg} - \frac{1}{4} \Delta \hat{N}_{if} \Delta \hat{N}_{jg} \right). \end{aligned} \quad (6)$$

It is expected that the exchange interaction occurs in the subsystem of quasi-localized states only between the nearest neighbors both in the xy plane and along the z axis. This is reflected in the equation through the inclusion of the indices of sites f and g at the summation sign in angle brackets. In this expression, each of the operators describes the deviations from its mean value by equation $\Delta \hat{A} = \hat{A} - \langle \hat{A} \rangle$. \mathbf{S}_{jm} is the quasi-spin vector operator of the localized subsystem, the components of which are associated with the operators of atomic representation by the equations $S_{jm}^+ = X_{jm}^{\uparrow\downarrow}$, $S_{jm}^- = X_{jm}^{\downarrow\uparrow}$, $S_{jf}^z = \sum_{\sigma} (\eta_{\sigma}/2) X_{jf}^{\sigma\sigma}$. The operator of the number of localized electrons at site f is determined as $\hat{N}_{jf} = \sum_{\sigma} X_{jf}^{\sigma\sigma}$.

We will use the Matsubara Green's functions in the atomic representation, which in general terms are determined from equation

$$D_{\gamma, \nu}^{AA'}(x - x') = -\langle T_{\tau} \tilde{X}^{\gamma}(x) \tilde{X}^{-\nu}(x') \rangle, \quad (7)$$

where $x = (\mathbf{R}_m, \tau)$ is the four-dimensional coordinate including three spatial coordinates of \mathbf{R}_m and imaginary time τ , and ν and γ are the root vectors for the Hubbard operators. The root vector uniquely determines the original pair index (n, n') of the Hubbard operator, so it is often designed as $\gamma(n, n')$. The dimension of the root vector coincides with the dimension of the basis of atomic states, and the i th component of the root vector is written in a simple universal form as

$\gamma_i(n, n') = \delta_{in} - \delta_{in'}$. The advantages of introducing the root vectors are described in detail [22]. The superscript A indicates the affiliation of the spatial coordinates \mathbf{R}_m of the Hubbard operator taking the first position in the definition of Green's function to a particular sublattice; that is, $A \equiv F$, if $\mathbf{R}_m = \mathbf{R}_f$, and $A \equiv G$, if $\mathbf{R}_m = \mathbf{R}_g$. Similarly, index A' uniquely determines to which sublattice the second operator of Green's function belongs. The definition of Green's function includes the Hubbard operators in the Heisenberg representation, that is, $\tilde{X}^\gamma(x) = \exp(\tau\hat{H})X_m^\gamma\exp(-\tau\hat{H})$. The angle brackets in Eq. (7) mean thermodynamic averaging with the density matrix $\exp(-\beta\hat{H})/\text{Sp}[\exp(-\beta\hat{H})]$, in which $\beta = 1/T$ is the inverse temperature (hereinafter, the temperature is measured in energy units). The standard transition to the interaction, wherein $X^\gamma(x) = \exp(\tau\hat{H}_0)X_m^\gamma\exp(-\tau\hat{H}_0)$, leads to Green's function taking the form

$$D_{\gamma,\nu}^{AA'}(x-x') = -\langle T_\tau X^\gamma(x)X^{-\nu}(x')S(\beta) \rangle_0 / \langle S(\beta) \rangle_0, \quad (8)$$

where $S(\beta) = T_\tau \exp\left[-\int_0^\beta d\tau \hat{H}_{\text{int}}(\tau)\right]$ is the scattering matrix and $\hat{H}_{\text{int}} = \hat{H}_{\text{mix}} + \hat{H}_{\text{exch}}$. The Fourier transformation and expansion over quasi-momenta of the Matsubara Green's function can be written as

$$D_{\gamma,\nu}^{AA'}(x-x') = \frac{T}{N} \sum_{\mathbf{q}, \omega_m} \exp[i\mathbf{q}(\mathbf{R}_m - \mathbf{R}_{m'}) - i\omega_m(\tau - \tau')] D_{\gamma,\nu}^{AA'}(\mathbf{q}, i\omega_m). \quad (9)$$

Further, it is convenient to use the four-dimensional vector $q = (\mathbf{q}, i\omega_m)$.

The problem of finding the temperature dependence of the antiferromagnetic order parameter is reduced to determination of the Fourier transform $D_{\uparrow\downarrow,\uparrow\downarrow}^{F_j F_j}(q)$ in the expansion of the scattering matrix into a series. The designation F_j is introduced to show that Green's function is based on operators belonging to the F sublattice and related to the j plane of the unit cell. The difficulties in solving this problem are connected in a general way to the need to describe a quasi-two-dimensional structure with two sublattices and to consider simultaneously exchange and hybridization interactions. It is expected that the exchange interaction between localized electrons is responsible for long-range antiferromagnetic order. If the localized level is completely full (the Fermi level lies above the f level), the system is close to the behavior of a Heisenberg antiferromagnet in terms of magnetic properties. It is believed that when a localized level is partially filled, the main effects determining the temperature dependence of the antiferromagnetic order parameter

are caused by hybridization processes. In this regard, for the qualitative study of the impact of hybridization on the main characteristics of a heavy-fermion antiferromagnet, such as spin-wave stiffness, the antiferromagnetic order parameter, and the Néel temperature, it is sufficient to limit ourselves to the Tyablikov approximation when considering the "exchange" contributions to the quasi-spin Green's function [26]. This approximation can significantly simplify the Dyson equation for $D_{\uparrow\downarrow,\uparrow\downarrow}^{F_j F_j}(q)$.

It is convenient to introduce the matrix Green's function \hat{D}_\perp :

$$\hat{D}_\perp = \begin{bmatrix} D_{\uparrow\downarrow,\uparrow\downarrow}^{F_1 F_1} & D_{\uparrow\downarrow,\uparrow\downarrow}^{F_1 F_2} & D_{\uparrow\downarrow,\uparrow\downarrow}^{F_1 G_1} & D_{\uparrow\downarrow,\uparrow\downarrow}^{F_1 G_2} \\ D_{\uparrow\downarrow,\uparrow\downarrow}^{F_2 F_1} & D_{\uparrow\downarrow,\uparrow\downarrow}^{F_2 F_2} & D_{\uparrow\downarrow,\uparrow\downarrow}^{F_2 G_1} & D_{\uparrow\downarrow,\uparrow\downarrow}^{F_2 G_2} \\ D_{\uparrow\downarrow,\uparrow\downarrow}^{G_1 F_1} & D_{\uparrow\downarrow,\uparrow\downarrow}^{G_1 F_2} & D_{\uparrow\downarrow,\uparrow\downarrow}^{G_1 G_1} & D_{\uparrow\downarrow,\uparrow\downarrow}^{G_1 G_2} \\ D_{\uparrow\downarrow,\uparrow\downarrow}^{G_2 F_1} & D_{\uparrow\downarrow,\uparrow\downarrow}^{G_2 F_2} & D_{\uparrow\downarrow,\uparrow\downarrow}^{G_2 G_1} & D_{\uparrow\downarrow,\uparrow\downarrow}^{G_2 G_2} \end{bmatrix}. \quad (10)$$

It is known that the matrix Green's function decomposes into the product of $\hat{D}_\perp = \hat{G}_\perp \hat{P}$, where \hat{P} is a component matrix of the force operator [27]. The equation for finding the matrix function \hat{G}_\perp can be represented as

$$\hat{G}_\perp = \hat{G}_\perp^{(0)} + \hat{G}_\perp^{(0)} \hat{\Sigma} \hat{G}_\perp, \quad \hat{G}_\perp^{(0)} = \hat{G}^{(0)} + \hat{G}^{(0)} \hat{P} \hat{I} \hat{G}_\perp^{(0)}. \quad (11)$$

The graphic form of Eq. (11) is shown in Fig. 1. The thick solid line indicates the desired matrix function \hat{G}_\perp . The dashed line corresponds to a diagonal matrix $\hat{G}^{(0)}$, the components of which determine the bare quasi-spin Green's function for the F - and G sublattices, respectively: $G_0^{F_j F_j}(i\omega_m) = (i\omega_m - 2\tilde{h})^{-1}$, $G_0^{G_j G_j}(i\omega_m) = (i\omega_m + 2\tilde{h})^{-1}$, where $\tilde{h} = (J_0 + K_0)R/2$. The wavy line determines the interaction matrix \hat{I} , which includes the Fourier transforms of the exchange integrals. In the applied approximation of nearest neighbors, the exchange interaction matrix \hat{I} can be represented as

$$\hat{I} = \frac{1}{2} \begin{bmatrix} 0 & 0 & J_q & K_q \\ 0 & 0 & K_q & J_q \\ J_q & K_q & 0 & 0 \\ K_q & J_q & 0 & 0 \end{bmatrix}, \quad (12)$$

where $J_q = 4J \cos(q_x b/2) \cos(q_y b/2)$, $K_q = 2K \cos(q_z c/2)$.

The graphic element in the form of a circle in Fig. 1 corresponds to the matrix $\hat{\Sigma}$, containing the components of a mass operator irreducible by the Larkin method [28]. Only corrections for the hybridization interaction are taken into account in the mass operator. The "triangle" in Fig. 1 is the matrix \hat{P} with the

components of the force operator, which take into account both the bare end factors of the spin Green's function and corrections related to the hybridization interaction.

Because the processes of the hopping and hybridization of electrons are limited by the xy plane, $\Sigma^{A_j B_j}$, $P^{A_j B_j}$, are the nonzero components of the mass and force operators, where $A, B = F, G$ and components with various j are equal to each other. In this regard, the subscript j can be omitted. We introduce convenient designations $d_{AB} = \Sigma^{AB} + J_q \delta P^{AB} / 2$, $K_{AB} = K_q \delta P^{AB} / 2$, $\bar{F} \equiv G, \bar{G} \equiv F$ (for brevity, the dependence

on q of the components of the mass and force operators is not specified). The values of d_{AB} in this approach are analogues of the components of the mass operator irreducible by Dyson. The appearance of additional terms K_{AB} is due to the quasi-two-dimensional structure of the lattice. As previously noted, in the components FF and GG of the force operator, both the bare end Heisenberg factors and the corrections caused by the hybridization interaction, that is, $P^{FF} = 2R + \delta P^{FF}$, $P^{GG} = -2R + \delta P^{GG}$, are taken into account. Consideration of the mass and force operators leads to the following expression for the inverse matrix:

$$\hat{G}_{\perp}^{-1} = \begin{bmatrix} i\omega_m - 2\tilde{h} - d_{FF} & -K_{FG} & -J_q R - d_{FG} & -K_q R - K_{FF} \\ -K_{FG} & i\omega_m - 2\tilde{h} - d_{FF} & -K_q R - K_{FF} & -J_q R - d_{FG} \\ J_q R - d_{GF} & K_q R - K_{GG} & i\omega_m + 2\tilde{h} - d_{GG} & -K_{GF} \\ K_q R - K_{GG} & J_q R - d_{GF} & -K_{GF} & i\omega_m + 2\tilde{h} - d_{GG} \end{bmatrix}. \quad (13)$$

Then, the denominator of the Green's functions, determining the spin-wave spectrum, can be written as

$$\Delta(q) = \begin{bmatrix} (i\omega_m - 2\tilde{h} - d_{FF} - K_{FG})(i\omega_m + 2\tilde{h} - d_{GG} - K_{GF}) \\ + (J_q R + K_q R + K_{FF} + d_{FG})(J_q R + K_q R - K_{GG} - d_{GF}) \end{bmatrix} \times \begin{bmatrix} (i\omega_m - 2\tilde{h} - d_{FF} + K_{FG})(i\omega_m + 2\tilde{h} - d_{GG} + K_{GF}) \\ + (K_q R - J_q R + K_{FF} - d_{FG})(K_q R - J_q R - K_{GG} + d_{GF}) \end{bmatrix}. \quad (14)$$

Let us limit the consideration of the contributions of the hybridization interaction to the mass and force operators by the one-loop approximation. Then, arbitrary component AA' of the mass operator $\hat{\Sigma}$ is determined by two graphs that characterize the processes of magnon decay into separate fermions from different electronic subsystems. These diagrams are presented in Fig. 2. The solid lines with two bold clear or solid arrows \triangleright , \blacktriangleright denote the propagators of localized electrons with the projection of the spin momentum \uparrow and \downarrow , respectively. One of four propagators of localized electrons, designated by index AA' , enters each com-

ponent of the mass operator. A solid line with two thin arrows $>$ represents any of the four propagators for the Bogolyubov operators $\alpha_{p\sigma}, \beta_{p\sigma}$, describing the itinerant electron subsystem. Thus, each graph is represented as a sum of four diagrams. The intersection of the three Green's functions indicates hybridization interaction at this point. The exact form of the interaction parameter is easily restored with the help of the matrix representation of the Hamiltonian (Eq. (4)). The graphs also present four-dimensional momenta p and q . Summation occurs by the internal momenta p . It is

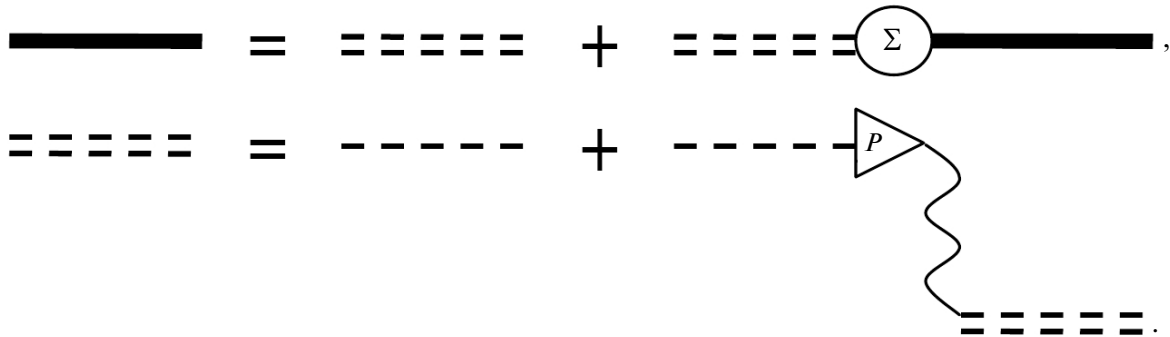


Fig. 1. Dyson equation for the matrix Green's spin function.

easily seen that 32 diagrams for the components of the mass operator can be obtained from the above figures.

For the components of the force operator, in addition to the bare end factors, 32 diagrams are also introduced (Fig. 3). A solid line with a bold arrow \triangleright (or \blacktriangleright) denotes the bare Green's function of localized electrons with the spin \uparrow (\downarrow). Symbols \circ , \bullet represent the end Hubbard factors for the respective directions of the electron spin.

The analytical expression for the FF component of the mass operator, obtained from Fig. 2, is

$$\begin{aligned} \Sigma^{FF}(q) = & -\frac{T}{2N} \sum_{p\sigma} \eta_{\sigma} G_{\sigma}^{FF}(p + \eta_{\sigma} q) \\ & \times \left[(V_p + W_p)^2 G_{\sigma}^{\alpha\alpha}(p) + (V_p - W_p)^2 \right. \\ & \left. \times G_{\sigma}^{\beta\beta}(p) + (W_p^2 - V_p^2) (G_{\sigma}^{\alpha\beta}(p) + G_{\sigma}^{\beta\alpha}(p)) \right]. \end{aligned} \quad (15)$$

With the matrix representation used in the notation of the Hamiltonian \hat{H}_{mix} , the matrix Matsubara Green's function \hat{D}_{σ} can be introduced, which determines the

propagators of itinerant and localized electrons. The definition for the electron Matsubara function is

$$\begin{aligned} & -\left\langle T_{\tau} \hat{C}_{p\sigma,i}(\tau) \hat{C}_{p\sigma,j}^{\dagger}(\tau') S(\beta) \right\rangle_0 \\ & = T \sum_{\omega_n} \exp[-i\omega_n(\tau - \tau')] \left(\hat{D}_{\sigma} \right)_{ij}, \end{aligned} \quad (16)$$

where \hat{D}_{σ} is the matrix representation of Fourier transforms of the normal electron Green's functions. Each component $\left(\hat{D}_{\sigma} \right)_{ij}$ depends on the coordinate of $p = (\mathbf{p}, i\omega_n)$. As before, it is convenient to present the full Green's matrix function in the form of a matrix product of the propagator and the force operator, that is, $\hat{D}_{\sigma} = \hat{G}_{\sigma} \hat{P}_{\sigma}$.

The propagators of localized and itinerant electrons will be calculated in the Hubbard-I approximation. In this approximation, let us derive the inverse matrix to \hat{G}_{σ} , from which it is easy to find any of the electron propagators:

$$\hat{G}_{\sigma}^{-1} = \begin{bmatrix} i\omega_n - \xi_{\alpha p} & 0 & -\tilde{V}_p - \tilde{W}_p & -\tilde{V}_p - \tilde{W}_p \\ 0 & i\omega_n - \xi_{\beta p} & \tilde{V}_p - \tilde{W}_p & \tilde{W}_p - \tilde{V}_p \\ -N_{0\sigma}(\tilde{V}_p + \tilde{W}_p) & N_{0\sigma}(\tilde{V}_p - \tilde{W}_p) & i\omega_n - \xi_{\sigma}^F & 0 \\ -N_{0\bar{\sigma}}(\tilde{V}_p + \tilde{W}_p) & N_{0\bar{\sigma}}(\tilde{W}_p - \tilde{V}_p) & 0 & i\omega_n - \xi_{\sigma}^G \end{bmatrix}, \quad (17)$$

where $\tilde{V}_p = V_p/\sqrt{2}$, $\tilde{W}_p = W_p/\sqrt{2}$. The determinant of the inverse matrix determines the hybridization electron spectrum in the antiferromagnetic phase. In the Hubbard-I approximation, the matrix of the electronic force operator is diagonal with elements $[1 \ 1 \ N_{0\sigma} \ N_{0\bar{\sigma}}]$ along the main diagonal, where $N_{0\sigma} = 1 - n_L/2 + \eta_{\sigma} R$.

RESULTS AND DISCUSSION

Spectrum of spin-wave excitations. To account for the main contribution that determines the renormalization of the spectrum of spin-wave excitations, we restrict ourselves to hybridization corrections in the first approximation. Then, the solutions of the dispersion equation $\Delta(q) = 0$ (Eq. (14)), obtained after analytical continuation, has the form

$$\omega_{iq} = \omega_{0i}(\mathbf{q}) + \delta\omega_{iq}, \quad (i = 1, 2), \quad (18)$$

which corresponds to the two branches of the spectrum of spin-wave excitations taking into account the quasi-two-dimensional structure. Here, we introduced the following designations:

$$\omega_{01,2}(\mathbf{q}) = R \sqrt{(J_0 + K_0)^2 - (J_q \pm K_q)^2}, \quad (19)$$

$$\begin{aligned} \delta\omega_{1,2q} = & \frac{1}{2} [d_{1,2FF} + d_{1,2GG} \pm (K_{1,2FG} + K_{1,2GF})] \\ & - \frac{1}{2\omega_{01,2}(\mathbf{q})} \{ (J_0 + K_0) R [d_{1,2GG} - d_{1,2FF} \\ & \pm (K_{1,2GF} - K_{1,2FG})] + (J_q \pm K_q) \\ & \times R [d_{1,2FG} - d_{1,2GF} \pm (K_{1,2FF} - K_{1,2GG})] \}, \end{aligned} \quad (20)$$

where $\omega_{01,2}(\mathbf{q})$ is the bare magnon spectrum without hybridization interaction, and $\delta\omega_{1,2q}$ is corrections due to hybridization. The appearance of the acoustic and optical branches of the magnon spectrum is caused by the different nature of the rotation of the spin momenta at the nearest sites along the z axis, taking into account the quasi-two-dimensionality of the antiferromagnet: in phase and in antiphase, respectively [29, 30]. The positive sign in Eqs. (19) and (20) corresponds to the Goldstone branch, designated by index 1, and the negative sign is for the branch with index 2, the excitations of which are separated by a gap. The designations $d_{iAB} = d_{AB}(\omega_{0i}(\mathbf{q}))$, $K_{iAB} = K_{AB}(\omega_{0i}(\mathbf{q}))$ indicates that all components of the mass and force operators are calculated for the corresponding initial energy of magnons.

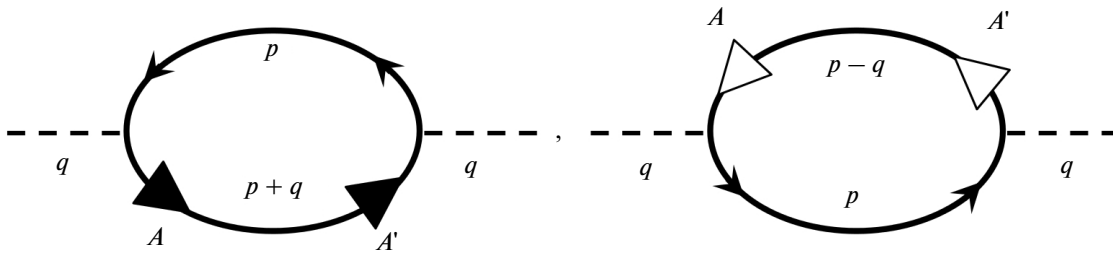


Fig. 2. Diagrams for the components of the mass operator.

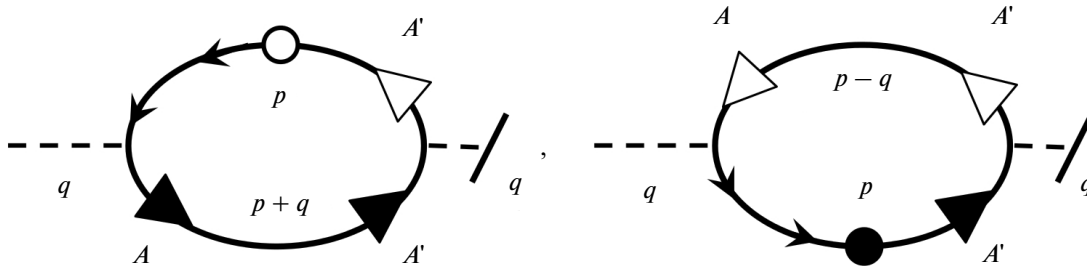


Fig. 3. Diagrams for the components of the force operator.

The dependences of the branches of the spin-wave spectrum on the component of the wave vector q_α along the main direction of the magnetic Brillouin zone ($\alpha = x, y, z$, a_α is the parameter of the unit cell along the respective axis) are shown by solid and dashed lines (Fig. 4) for a quasi-two-dimensional lat-

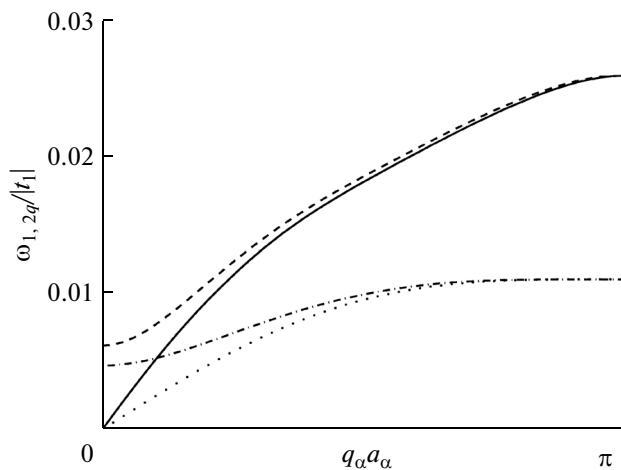


Fig. 4. Spectrum of spin-wave excitations of the quasi-two-dimensional structure along the main direction of the magnetic Brillouin zone, taking into account (solid and dashed lines) hybridization and (dotted and dash-dotted lines) the bare spectrum; $n_e = 1.2$; $V = 0.3$; $E_0 = -2$; $J = 0.008$; $K = J/10$; the energy is given in units of $|t_1|$, where t_1 is the hopping amplitude of itinerant electrons between neighboring sites.

tice taking into account the hybridization interaction between localized and itinerant electrons. For comparison, the dotted and dash-dotted lines show the branches of the bare spectrum of spin-wave excitations of localized electrons without hybridization. The bare localized level lies in the middle of the lower antiferromagnetic subband of the Fermi spectrum; the total concentration of electrons in the system is fixed at $n_e = 1.2$; and the exchange parameters $J = 0.008|t_1|$ (t_1 is the hopping amplitude of itinerant electrons between neighboring sites) and $K = J/10$. The value of $|t_1|$ in cerium heavy-fermion compounds is estimated on the basis of the ab-initio calculations and is 0.1–0.3 eV. The parameters are selected so that the chemical potential crosses the low dispersion band of heavy fermions, separated from the remaining bands by the hybridization and antiferromagnetic gaps [31, 32]. It is seen that taking into account hybridization processes with the intensity $V = 0.3|t_1|$ leads to an increase in the spin-wave stiffness for the acoustic branch and an increase in the energy of spin excitations.

An increase in the magnon energy in the periodic Anderson model in comparison with the Heisenberg regime is because the consideration of hybridization corrections results in an additional mechanism for the effective exchange interaction between localized electrons along with the interaction which is taken into account in the Hamiltonian $\widehat{H}_{\text{exch}}$. The components of the mass operator may both promote the initial antiferromagnetic ordering of localized electrons and sup-

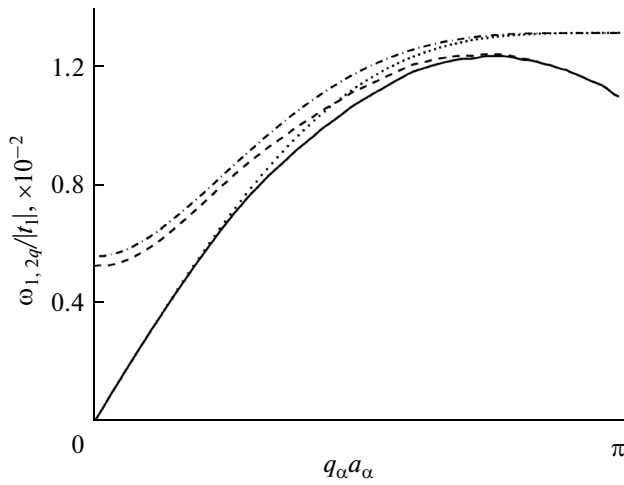


Fig. 5. Spectrum of spin-wave excitations of the quasi-two-dimensional structure along the main direction of the magnetic Brillouin zone, taking into account (solid and dashed lines) hybridization and (dotted and dash-dotted lines) the bare spectrum at an electron concentration of $n_e = 1.4$.

press it when the hybridization processes induce the ferromagnetic exchange interaction. The hybridization corrections to the force operators lead to renormalization of the bare end factors determined by the antiferromagnetic order parameter.

Qualitatively different behavior of the magnon spectrum is demonstrated in Fig. 5, when the concentration increased to $n_e = 1.4$. In this case, the quasi-localized electronic subsystem is almost full. It is seen from Fig. 5 that the spin-wave stiffness for such parameters remains almost the same as for localized electrons. Upon the transition to the short wavelength region, the spin-wave excitation energy decreases, indicating the slight suppression of antiferromagnetism and a decrease in the value of the antiferromagnetic order parameter due to hybridization.

Temperature dependence of the antiferromagnetic order parameter. The expression for the antiferromag-

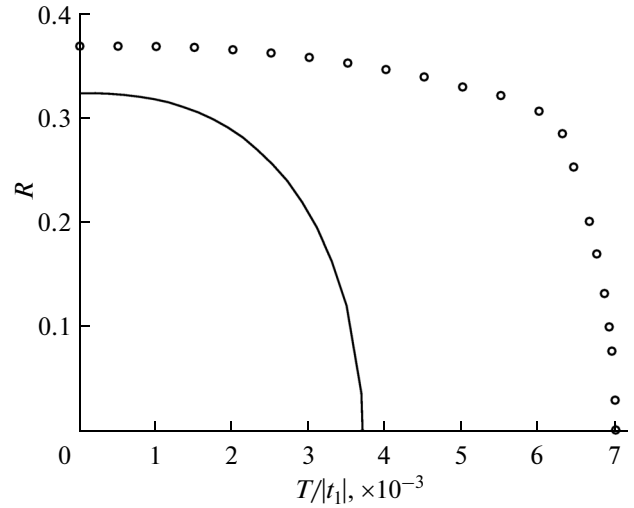


Fig. 6. Dependence of the antiferromagnetic order parameter on temperature for the quasi-two-dimensional structure, taking (points) and not taking (solid line) hybridization processes into account; parameters are the same as in Fig. 4.

netic order parameter is given in the form of $R = n_L/2 - \langle X_{1f}^{\downarrow\downarrow} \rangle$, in which the number of filling in the quasi-localized subsystem of Hubbard fermions is related to the Fourier transform of the quasi-spin Green's function by equation

$$\langle X_{1f}^{\downarrow\downarrow} \rangle = -\frac{T}{N} \sum_q \exp[-i\omega_n \delta] D_{\uparrow\downarrow, \uparrow\downarrow}^{F_1 F_1}(q). \quad (21)$$

In deriving the last equation, it was assumed that the spin degrees of freedom played a decisive role in the formation of magnetic ordering. The analytical form of the Green's function, included in Eq. (21), can be easily obtained with the help of matrix (13).

The following equation was obtained for the antiferromagnetic order parameter, corresponding to the approximation within which the magnon spectrum was previously calculated,

$$R = \frac{n_L/2}{\sum_q \left[\frac{2\tilde{\hbar}}{\omega_{1q}} \operatorname{cth}\left(\frac{\omega_{1q}}{2T}\right) + \frac{2\tilde{\hbar}}{\omega_{2q}} \operatorname{cth}\left(\frac{\omega_{2q}}{2T}\right) \right] \left(1 + \frac{2J_q K_q R^2}{\omega_{1q}^2 - \omega_{2q}^2} \right) + C + \sum_{q,i=1,2} \frac{\Theta_{iq}}{\exp[\omega_{iq}/T] - 1}}. \quad (22)$$

The designations of C and Θ_{iq} contain only corrections related to the hybridization interaction. In the limit of $V \rightarrow 0$, $n_L \rightarrow 1$ the equation becomes an equation for a Heisenberg quasi-two-dimensional antiferromagnet [15], as $\omega_{iq} \rightarrow \omega_{0i}(\mathbf{q})$. The appearance of parameter n_L in the numerator of Eq. (22) is due to the possibility of the consideration of partial filling of the quasi-localized level. It is shown that the main contri-

butions that determine the antiferromagnetic order parameter are associated with renormalization of the energy of spin-wave excitations in accounting for hybridization (Figs. 4 and 5).

The temperature dependence of the antiferromagnetic order parameter is presented in Fig. 6. The points represent the results of numerical calculation in the consideration of hybridization processes. The solid line indicates the dependence obtained without hybridization.

The same parameters as in Fig. 4 are selected. It is seen that the inclusion of hybridization corrections renormalizes both the antiferromagnetic order parameter and the Néel temperature. The hybridization interaction facilitates antiferromagnetism, resulting in an increase in the values of $R(0)$ and T_N . The Néel temperature increases most pronouncedly.

The obtained dependence indicates that the processes of hybridization between localized and itinerant electrons should be taken into account in the description of the experimental data for cerium-based heavy-fermion intermetallic compounds in the antiferromagnetic and mixed phases and in estimation of the effective exchange parameters.

Mixed phase of superconductivity and antiferromagnetism with broken time-reversal symmetry. Previously, based on the analysis of equations of the Gor'kov type for the mixed phase of superconductivity and antiferromagnetism of heavy-fermion systems, in which the symmetry is spontaneously broken with respect to time reversal, it was shown that the presence of antiferromagnetic ordering leads to the significant modification of the superconducting order parameter [19]. The formation of the Cooper instability does not affect the antiferromagnetism. Therefore, knowledge of the dependence of magnetization $R(T)$ of the antiferromagnetic sublattice on temperature determines fully the behavior of the superconducting order parameter in the mixed phase and enables the critical temperature of occurrence of the Cooper instability in the presence of antiferromagnetism to be found.

For the model described by the Hamiltonian (1), the Cooper instability is induced by the exchange interaction (Eq. (6)) in the subsystem of quasi-localized electrons. It is believed that the presence of exchange along the z axis does not affect the Cooper pairing that develops in the xy plane. The equation for determining the amplitude Δ_d of the superconducting order parameter of d -wave symmetry, obtained in the Hubbard-I approximation, with the known dependence of $R(T)$ is

$$\begin{aligned} \Delta_d = & 2J\Delta_d \sum_{\mathbf{k}} \left[\sin\left(\frac{k_x b}{2}\right) \sin\left(\frac{k_y b}{2}\right) \right]^2 \\ & \times \sum_{j=1, \dots, 4} \frac{Q_{\mathbf{k}}(E_{j\mathbf{k}}) \text{th}(E_{j\mathbf{k}}/2T)}{2E_{j\mathbf{k}} \prod_{i \neq j} (E_{j\mathbf{k}}^2 - E_{i\mathbf{k}}^2)} \\ & - 8J\Delta_d^3 \sum_{\mathbf{k}} \left[\sin\left(\frac{k_x b}{2}\right) \sin\left(\frac{k_y b}{2}\right) \right]^4 \\ & \times \sum_{j=1, \dots, 4} \frac{S_{\mathbf{k}}(E_{j\mathbf{k}}) \text{th}(E_{j\mathbf{k}}/2T)}{2E_{j\mathbf{k}} \prod_{i \neq j} (E_{j\mathbf{k}}^2 - E_{i\mathbf{k}}^2)}, \end{aligned} \quad (23)$$

where $E_{j\mathbf{p}}$ are the branches of the spectrum of Fermi excitations in the mixed phase [33],

$$\begin{aligned} Q_{\mathbf{p}}(\omega) = & \sum_{\sigma=\uparrow, \downarrow} \left[(\omega - \xi_{\sigma}^F) \left((\omega - \xi_{\mathbf{p}})^2 - \Gamma_{\mathbf{p}}^2 \right) \right. \\ & \left. - N_{0\sigma} (\omega - \xi_{\mathbf{p}}) (V_{\mathbf{p}}^2 + W_{\mathbf{p}}^2) - 2N_{0\sigma} \Gamma_{\mathbf{p}} V_{\mathbf{p}} W_{\mathbf{p}} \right] \\ & \times \left[(\omega + \xi_{\sigma}^F) \left((\omega + \xi_{\mathbf{p}})^2 - \Gamma_{\mathbf{p}}^2 \right) - N_{0\sigma} (\omega + \xi_{\mathbf{p}}) \right. \\ & \left. \times (V_{\mathbf{p}}^2 + W_{\mathbf{p}}^2) + 2N_{0\sigma} \Gamma_{\mathbf{p}} V_{\mathbf{p}} W_{\mathbf{p}} \right] \\ & + N_{0\sigma}^2 \left[2(\omega - \xi_{\mathbf{p}}) V_{\mathbf{p}} W_{\mathbf{p}} + \Gamma_{\mathbf{p}} (V_{\mathbf{p}}^2 + W_{\mathbf{p}}^2) \right] \\ & \times \left[2(\omega + \xi_{\mathbf{p}}) V_{\mathbf{p}} W_{\mathbf{p}} - \Gamma_{\mathbf{p}} (V_{\mathbf{p}}^2 + W_{\mathbf{p}}^2) \right], \\ S_{\mathbf{p}}(\omega) = & \frac{2 \left((1 - n_L/2)^2 + R^2 \right)}{\left((1 - n_L/2)^2 - R^2 \right)^2} \\ & \times \left((\omega - \xi_{\mathbf{p}})^2 - \Gamma_{\mathbf{p}}^2 \right) \left((\omega + \xi_{\mathbf{p}})^2 - \Gamma_{\mathbf{p}}^2 \right). \end{aligned} \quad (24)$$

The antiferromagnetic order parameter R is included in the function of $Q_{\mathbf{p}}(\omega)$ by means of the average exchange field which renormalizes the energy of localized electrons in the paramagnetic phase and the bare end Hubbard factors $N_{0\sigma}$ of electrons in the antiferromagnetic phase. It is easy to show that Eq. (23) has a solution at $T = T_c$ and $\Delta_d = 0$ and determines the superconductivity temperature T_c . Thus, knowing the dependence of $R(T)$ for the quasi-two-dimensional structure taking into account the processes of hybridization, it is easy to determine the critical temperature and the temperature dependence of the superconducting order parameter in the mixed phase of cerium-based heavy-fermion intermetallic compounds.

CONCLUSIONS

In the framework of the extended periodic Anderson model, explicitly taking into account the exchange interaction between localized momenta, we analyzed the effect of low-energy processes of the hybridization of localized and itinerant states on the spectrum of spin-wave excitations, the order parameter, and the critical temperature in the antiferromagnetic and mixed phases of quasi-two-dimensional cerium-based intermetallic compounds such as CeRhIn₅. To solve this problem, corrections to the components of the mass and force operators of the Matsubara spin Green's function, related to the hybridization interaction, were considered. It is shown that taking into account the mixing of itinerant and localized electrons leads to a marked change in the Néel temperature. This is because hybridization induces further effective exchange interaction in the subsystem of localized electrons, which not only facilitates the original antiferromagnetic ordering but also suppresses antiferromagnetism. Simultaneous consideration of the

hybridization processes and the quasi-two-dimensional nature of the electronic structure significantly normalizes the temperature dependence of the superconducting and antiferromagnetic order parameters and the critical temperatures at which antiferromagnetism and superconductivity appear in the broken time-reversal symmetry phase. The above factors allowed determination of the temperature of the transition to the mixed phase, which agrees well with the experimental data for CeRhIn₅.

ACKNOWLEDGMENTS

The work is supported by the Russian Foundation for Basic Research, project nos. 13-02-00523 and 15-42-04372. A.O. Zlotnikov is also grateful for the Grant Program for Young PhDs supported by the President of the Russian Federation, project no. SP-1370.2015.5.

REFERENCES

1. A. I. Buzdin, L. N. Bulaevskii, M. L. Kulich, and S. V. Panyukov, *Sov. Phys. Usp.* **27**, 927 (1984).
2. W. Baltensperger and S. Strassler, *Phys. Condens. Matter.* **1**, 20 (1963).
3. C. Pfleiderer, *Rev. Mod. Phys.* **81**, 1551 (2009).
4. J. D. Thompson and Z. Fisk, *J. Phys. Soc. Jpn.* **81**, 011002 (2012).
5. Y.-M. Lu and Z. Wang, *Phys. Rev. Lett.* **110**, 096403 (2013).
6. M. Ezawa, *Phys. Rev. Lett.* **114**, 056403 (2015).
7. H. Hegger, C. Petrovic, E. G. Moshopoulou, M. F. Hundley, J. L. Sarrao, Z. Fisk, and J. D. Thompson, *Phys. Rev. Lett.* **84**, 4986 (2000).
8. S. Kawasaki, T. Mito, Y. Kawasaki, G.-q. Zheng, Y. Kitaoka, D. Aoki, Y. Haga, and Y. Onuki, *J. Magn. Mater.* **272–276**, E19 (2004).
9. A. Llobet, J. S. Gardner, E. G. Moshopoulou, J.-M. Mignot, M. Nicklas, W. Bao, N. O. Moreno, P. G. Pagliuso, I. N. Goncharenko, J. L. Sarrao, and J. D. Thompson, *Phys. Rev. B* **69**, 024403 (2004).
10. K. Miyake, S. Schmitt-Rink, and C. M. Varma, *Phys. Rev. B* **34**, 6554 (1986).
11. P. Monthoux and G. G. Lonzarich, *Phys. Rev. B* **63**, 054529 (2001).
12. K. Miyake and Sh. Watanabe, *J. Phys. Soc. Jpn.* **83**, 061006 (2014).
13. P. Gegenwart, Q. Si, and F. Steglich, *Nature Phys.* **4**, 186 (2008).
14. W. Wu and A.-M.-S. Tremblay, *Phys. Rev. X* **5**, 011019 (2015).
15. V. V. Val'kov and A. D. Fedoseev, *Theor. Math. Phys.* **168**, 1216 (2011).
16. P. Das, S.-Z. Lin, N. J. Ghimire, K. Huang, F. Ronning, E. D. Bauer, J. D. Thompson, C. D. Batista, G. Ehlers, and M. Janoschek, *Phys. Rev. Lett.* **113**, 246403 (2014).
17. H. J. Leder and B. Muhlschlegel, *Z. Phys. B* **29**, 341 (1978).
18. V. V. Val'kov and D. M. Dzebisashvili, *Theor. Math. Phys.* **157**, 1565 (2008).
19. V. V. Val'kov and A. O. Zlotnikov, *JETP Lett.* **95**, 350 (2012).
20. V. V. Val'kov and A. O. Zlotnikov, *J. Supercond. Nov. Magn.* **26**, 2885 (2013).
21. R. O. Zaitsev, *Diagrammatic method in the theory superconductivity and ferromagnetism* (Moscow URSS, 2004) [in English].
22. S. G. Ovchinnikov and V. V. Val'kov, *Hubbard Operators in the Theory of Strongly Correlated Electrons* (Imperial College Press, London-Singapore, 2004) [in English].
23. P. D. Sacramento, *J. Phys.: Condens. Matter* **15**, 6285 (2003).
24. Yu. A. Izyumov and R. P. Ozerov, *Magnetic Neutronography* (Nauka, Moscow, 1966) [in Russian].
25. J. Hubbard, *Proc. R. Soc. A* **285**, 542 (1965).
26. Fu-cho Pu, *Sov. Phys. Dokl.* **5**, 128 (1960).
27. R. O. Zaitsev, *Sov. Phys. JETP* **41**, 100 (1975).
28. V. G. Bar'yakhtar, V. N. Kivoruchko, and D. A. Yablonskii, *Green Function Method in the Theory of Magnetism* (Naukova Dumka, Kiev, 1984) [in Russian].
29. S. G. Ovchinnikov and O. G. Petrakovskii, *Sov. Phys. Solid State* **29**, 1073 (1986).
30. S. M. Hayden, G. Aeppli, T. G. Perring, H. A. Mook, and F. Dogan, *Phys. Rev. B* **54**, R6905 (1996).
31. V. V. Val'kov and D. M. Dzebisashvili, *J. Exp. Theor. Phys.* **110**, 301 (2010).
32. V. V. Val'kov and A. O. Zlotnikov, *J. Exp. Theor. Phys.* **116**, 817 (2013).
33. V. V. Val'kov and A. O. Zlotnikov, *Theor. Math. Phys.* **174**, 421 (2013).

Translated by O. Zhukova